Available online at www.sciencedirect.com
SCIENCE DIRECT
Journal of Solid State Chemistry 179 (2006) 2027–2035
JOURNAL OF SOLID STATE CHEMISTRY
www.elsevier.com/locate/jssc

A controlled release of ibuprofen by systematically tailoring the morphology of mesoporous silica materials

Fengyu Qu[a,b], Guangshan Zhu[a,*], Huiming Lin[a], Weiwei Zhang[a], Jinyu Sun[a], Shougui Li[a], Shilun Qiu[a,*]

[a]*State Key Laboratory for Inorganic Synthesis and Preparative Chemistry, Jilin University, Changchun 130023, China*
[b]*Chemistry and Pharmaceutical College, Jiamusi University, Jiamusi 154007, China*

Received 16 December 2005; received in revised form 26 March 2006; accepted 2 April 2006
Available online 2 May 2006

Abstract

A series of mesoporous silica materials with similar pore sizes, different morphologies and variable pore geometries were prepared systematically. In order to control drug release, ibuprofen was employed as a model drug and the influence of morphology and pore geometry of mesoporous silica on drug release profiles was extensively studied. The mesoporous silica and drug-loaded samples were characterized by X-ray diffraction, Fourier transform IR spectroscopy, N_2 adsorption and desorption, scanning electron microscopy, and transmission electron microscopy. It was found that the drug-loading amount was directly correlated to the Brunauer–Emmett–Teller surface area, pore geometry, and pore volume; while the drug release profiles could be controlled by tailoring the morphologies of mesoporous silica carriers.

Keywords: Mesoporous silica; Morphology; Ibuprofen; Controlled release

1. Introduction

Controlled release technologies are becoming more and more important in modern medication and pharmaceuticals. Controlled drug release at a desired rate has numerous advantages over conventional forms of dosage: maintaining the patient's blood level, minimizing deleterious side effects, prolonging efficiency time, heightening bioavailability, improving patient compliance [1], protecting sensitive drugs from enzymatic or acidic degradation in the gastrointestinal tract, masking peculiar odors [2], etc.

Ibuprofen is a well-known non-steroidal anti-inflammatory drug and has been widely used for the treatment of inflammation, pain, or rheumatism. But this drug has a short biological half-life (2 h) [3], which makes it a suitable candidate for sustained or controlled drug delivery. Therefore, ibuprofen has been frequently employed as a model drug on the purpose of sustained/controlled release.

Recent reports in literature have demonstrated that mesoporous silica materials can be served as drug carrier systems [4–7], and several research groups have reported on the design of mesoporous silica-based carrier systems for sustained/controlled drug delivery [4,7,8–13]. It has been found that several factors may bring great influence on the drug release profiles from mesoporous silica carriers. The first factor is the pore size of mesoporous silica, or steric hindrance. It is generally accepted that the pore size has a pronounced influence on the kinetics of drug release. Horcajada and Andersson reported that drug delivery rate decreases with the decrease of the pore size [10,11]. The second one is the interaction of the host–guest, or the properties of mesoporous silica and the drug [8]. Muñoz et al. found that the increase of the affinity of the host–guest by suitable organically functionalized mesoporous silica could lead to slower drug release [9]. The third factor is pore geometry of mesoporous silica. It was shown that one-dimensional (1D) or three-dimensional (3D) "cage-like" pore structure with smaller pore openings of mesoporous silica is of great benefit to slow drug release

*Corresponding authors. Fax: +86 431 5168331.
E-mail address: sqiu@mail.jlu.edu.cn (S. Qiu).

0022-4596/$ - see front matter © 2006 Elsevier Inc. All rights reserved.
doi:10.1016/j.jssc.2006.04.002

[10]. Finally, the pH of dissolution media could affect drug delivery profiles as well [2].

To create suitable controlled formulation in vivo by using mesoporous silica materials, it is of great importance to comprehensively understand the drug delivery profiles from mesoporous silica and effectively manipulate drug delivery rate in vitro simulated body fluid (SBF).

Herein, we present an alternative method to control drug delivery profiles by systematically regulating the morphology of mesoporous silica materials. Since the pore size of MCM-41 and MCM-48 is large enough for "comfortable" entrapment of ibuprofen ($1.0 \times 0.5\,nm^2$) [7], and different pore geometries of mesoporous silica may influence drug delivery profiles as well, we selected a series of spherical and rope-like mesoporous silica with similar pore sizes (1.96–2.45 nm), variable pore geometries (hexagonal and cubic pore system), and the influence of the morphologies and pore geometries of mesoporous silica on drug delivery profiles in vitro has been extensively studied. In addition, all the samples were characterized by X-ray diffraction (XRD), Fourier transform IR (FTIR) spectroscopy, N_2 adsorption and desorption, scanning electron microscopy (SEM), and transmission electron microscopy (TEM).

2. Experimental section

2.1. Materials

All the reagents were used as they were received—without further purification: ibuprofen (Ibu, Tianzunzezhong, Chemical Co., Nanjing), cetyltrimethyammoniumbromide (CTAB, Huifeng Co., Shanghai), decaethyleneglycol monohexadecyl ether ($C_{16}EO_{10}$, Fluka), dodecyltrimethylammoniumbromide (DDAB, Aldrich), tetraethoxysiliane (TEOS, Tiantai Chemical Co., Tianjin), sodium silicate ($Na_2SiO_3 \cdot 9H_2O$, Yongqiang Medicine Chemical Co., Liaoning), ethyl acetate ($CH_3COOC_2H_5$, Tiantai Chemical Co., Tianjin).

2.2. Synthesis of mesoporous silica

The mesoporous silica MCM-41-A spheres were synthesized according to the previous report [4].

The MCM-41-B mesoporous silica sphere was synthesized according to published synthesis routes [14].

The synthesis of MCM-41-C was modified from the previous reports [15]. In a typical synthesis procedure, 0.42 g of DDAB and 0.75 mL of the 1 M sodium hydroxide solution were dissolved in 100 g of water–methanol (75/25 = w/w) solution. Then, 0.62 g of TEOS was added to the solution with vigorously stirring continuously for 8 h at room temperature, and then the resulting white precipitate was aged overnight. The white powder was then filtered out and extensively washed with distilled water, and then dried at 318 K for 72 h. The organic template (DDAB) was removed by calcination in air at 823 K for 6 h.

The mesoporous silica sphere MCM-41-D was synthesized using CTAB and $C_{16}EO_{10}$ as mixed surfactant template at ambient temperature as reported by Qi et al. [16].

MCM-48-E was synthesized by hydrothermal pathway similar to the procedure described by Monnier et al. [17]. Typically, a 20 mL of distilled water suspension in 4.0 g of CTAB was heated and vigorously stirred, and then 0.36 g of solid sodium hydroxide and 4.5 mL of TEOS were added. After the mixture was stirred for 2 h, the resulting white gel was sealed in a Teflon-lined stainless steel autoclave, heated at 373 K for 3 days under static condition. The white precipitate obtained was filtered out and washed extensively, and the as-synthesized sample was air-dried at room temperature overnight. The template was removed by calcination in air at 823 K for 5 h.

The rope-like MCM-41-F was synthesized by modified method from the previous literature report [18]. It was prepared directly in an autoclavable polypropylene bottle. A total of 19.6 g of CTAB followed by 10 g of solid Na_2SiO_3 were dissolved in 350 mL of distilled water. After the mixture became a clear solution, 15 g of ethyl acetate was quickly added under stirring. After being stirred for 30 min, the mixture was allowed to stand at ambient temperature for 5 h; then the mixture was kept at 363 K for 50 h in a heating bottle. During the ageing process, organic vapor was allowed to evanesce through the cap of the bottle. The resulting solid was recovered by the filtration of the still warm reaction mixture, extensively washed with distilled water and ethanol, and dried at ambient temperature. The template was removed by calcination at 823 K for 5 h in flowing air.

2.3. Drug loading and release

The loading of the drug was carried out by the immersion of calcined mesoporous silica samples in ibuprofen hexane solution with a certain concentration. A typical procedure for loading ibuprofen in MCM-41-A was as follows: 221 mg of calcined MCM-41-A was suspended in 10 mL of 0.1 M ibuprofen hexane solution under stirring for 2 h while preventing the evaporation of hexane. The drug-loaded sample was separated from the solution by vacuum filtration, washed with hexane until the filtrates reached 10 mL, and dried at room temperature. Filtrate (1.0 mL) was sucked and properly diluted to determine the drug-loading amount by UV-VIS spectrophotometer. The loading procedures for the other samples were the same as that of MCM-41-A. The drug-loaded samples were designated as Ibu/MCM-41-A, Ibu/MCM-41-B, Ibu/MCM-41-C, Ibu/MCM-41-D, Ibu/MCM-48-E, and Ibu/MCM-41-F, respectively. After the drug-loaded samples were compressed into tablet form with a diameter of 10 mm and a thickness of 0.5 mm, the release rate was obtained by soaking the drug-charged tablets (150 mg) in 500 mL of simulated proximal intestine fluid (pH = 6.8, buffer solution), maintained at a temperature of 310 K. At

predetermined time intervals, 3 mL samples were withdrawn and immediately replaced with an equal volume of dissolution medium to keep the volume constant. These samples were filtered (0.45 μm), properly diluted and analyzed for ibuprofen content at 222 nm using UV-VIS spectrophometer. All the experiments were performed in triplicate.

2.4. Characterization

Powder XRD data were collected on a SIEMENS D5005 diffractometer with Cu$K\alpha$ radiation at 40 kV and 30 mA. Nitrogen adsorption and desorption isotherm were measured using a Micromeritics ASAP 2010 M adsorptometer. Before measurement, the samples were degassed at 373 K for 12 h, and the measurements were obtained at 77 K. Specific surface areas and pore size distributions were calculated using the Brunauer–Emmett–Teller (BET) and Barrett–Joyner–Halenda (BJH) models from the adsorption branches, respectively. Particle morphology of these materials was determined by SEM micrographs using JEOL-JSM-6300 operating at an accelerating voltage of 20–30 kV. Samples were sputtered with a thin film of Pt. TEM images were recorded on JEOL 2010 F and Philips CM200 FEG with an acceleration voltage of 20 kV. An FTIR spectrometer (JASCOFT/IR-420) was used to record infrared spectra of mesoporous silica materials by the KBr method. Powdered materials were pressed into a tungsten mesh grid and installed in an in situ FTIR transmission cell, and the samples were outgassed in a vacuum system with a residue pressure of less than 3×10^{-4} Torr at ambient temperature. UV-VIS spectra were taken on a UV-2450, visible spectrophotometer, SHIMADZU.

3. Results and discussion

3.1. Characterization of samples

Fig. 1 represents the XRD diffraction patterns for as-synthesized, calcined, and corresponding drug-loaded samples. Each XRD pattern of the as-synthesized MCM-41-A and MCM-41-F (Fig. 1A and F) exhibits a strong [100] reflection peak with two small ones, which confirmed a highly ordered 2D hexagonal mesostructure (*p6m*). After the template was removed by calcination, the intensities of [100] diffractions were apparently increased, while the peak position was shifted to the high-angle region due to further condensation of SiOH under proper calcinations [19,20]. The XRD patterns of calcined MCM-41-B, MCM-41-C, and MCM-41-D showed only one low angle peak with a larger half-width (Fig. 1B–D), which can be indexed to (100) diffraction; while (110) and (200) peaks became ambiguous or disappeared, as usually observed for MCM-41 samples prepared from surfactants possessing short hydrocarbon chain (MCM-41-C) [11], or synthesis at low temperature and dilute solution [14–16], which indicated the mesoporous system has become disordered. The XRD patterns of the as-synthesized and calcined MCM-48-E samples are similar (Fig. 1E). They exhibit high intensity peaks (211) followed by a smaller one (220) at $2\theta = 2$–3°, whereas several other peaks are observed at $2\theta = 4$–8°. Such patterns correspond to the *Ia3d* cubic symmetry for MCM-48 type of mesoporous silica materials [21]. As shown in Fig. 1, each of the XRD patterns of Ibu/MCM-41-A, Ibu/MCM-41-B, Ibu/MCM-41-C, Ibu/MCM-41-D, and Ibu/MCM-41F sample shows only one (100) reflection, while the diffraction intensity decreased apparently upon loaded with the drug, which showed that the mesoporous phases have been maintained, while the integrity of mesopore structure was affected by the loading of the drug. The XRD pattern of Ibu/MCM-48-E exhibits a high intensity (211) peak and a low one (220), which confirmed that the cubic phase is still kept as the drug was loaded.

SEM was used to determine the particle size, particle morphology and the size distribution of the samples, and the detailed parameters were summarized in Table 1. As depicted in Fig. 2A–E the morphologies of MCM-41-A, MCM-41-B, MCM-41-C, MCM-41-D, and MCM-48-E are spherical, with average particle size of about 150, 500 nm, 1.25, 5 μm and 500 nm, respectively. The morphology of MCM-41-F is irregular rope-like with 5–10 μm in length (Fig. 2F). TEM study was performed to further determine pore geometry structure, showing that MCM-41-A and MCM-41-F possess ordered hexagonal pore systems (Fig. 3A and D), while MCM-41-B and MCM-41-C show worm-like pore structure (Fig. 3B and C). These observations were in agreement with the results of XRD patterns.

The FTIR spectra revealed that the SiOH band at 3744 cm^{-1} in mesoporous silica material disappears after ibuprofen was stored (Fig. 4). Meanwhile the intensities of ν (COOH) at 1723 cm^{-1} and δ_{oop} (OH) at 950 cm^{-1} of ibuprofen were decreased significantly [8,9]. This indicates the formation of a hydrogen bond between the carboxylic group of ibuprofen and the silanol group of the mesoporous silica. Moreover, that the quaternary carbon atom peaks at 1463 and 1519 cm^{-1}, and C–H_x peaks at 2919 and 2962 cm^{-1} (as clearly observed in the drug-loaded samples [22]) confirmed that the drug has been loaded in the mesoporous silica system.

Furthermore, the characteristics of calcined and drug-loaded samples were also confirmed by the results of nitrogen adsorption/desorption measurements (shown in Fig. 5), and the detailed data were summarized in Table 1. It was revealed that the samples possess high specific surface area and large pore volume. It can be observed that a well-defined step occurs in the adsorption curve at a relative pressure p/p^0 of 0.2–0.3 for all of the MCM-41-A, MCM-41-B, MCM-41-C, MCM-41-D, and MCM-48-E samples, indicating the filling of framework-confined mesopores [23]. The isotherms can be classified as type IV [24]. In addition, it could be observed that all the drug-loaded samples have the similar nitrogen adsorption/desorption curves compared with their corresponding

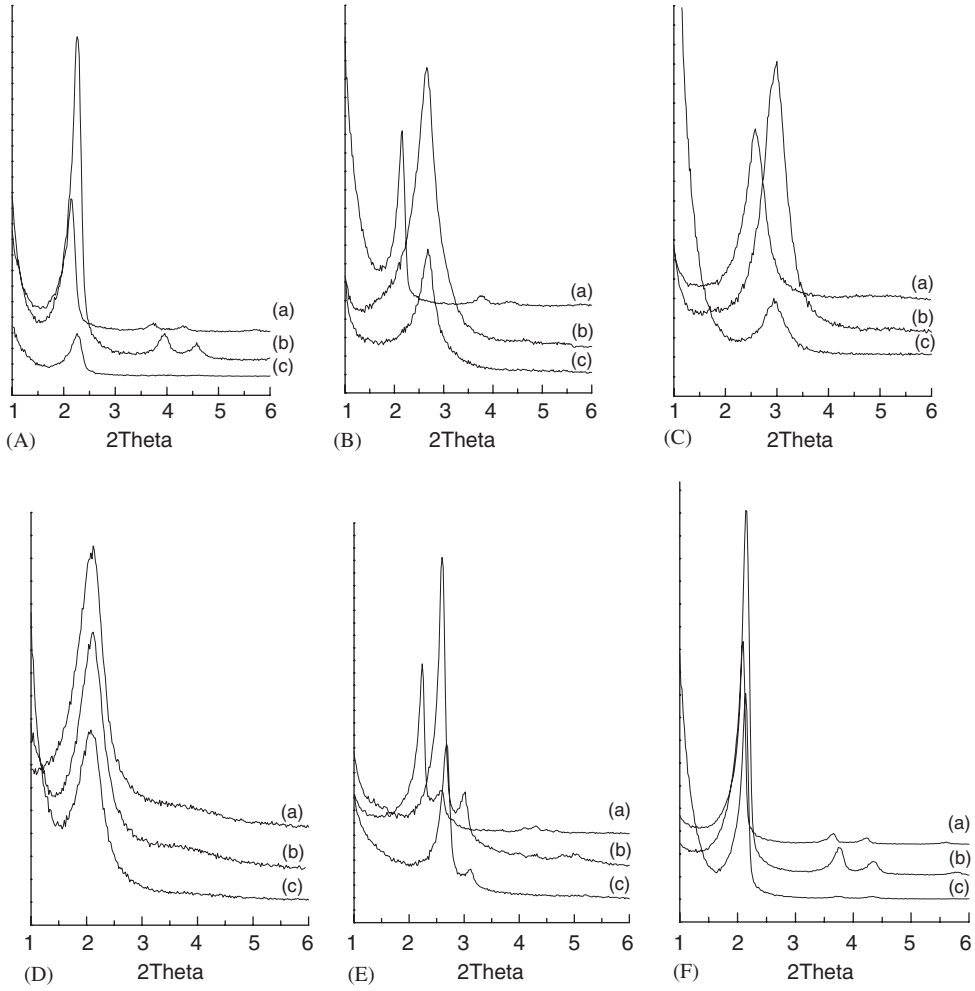

Fig. 1. The powder X-ray diffraction spectra of the samples: (A) MCM-41-A, (B) MCM-41-B, (C) MCM-41-C, (D) MCM-41-D, (E) MCM-48-E, (F) MCM-41-F; (a) as-synthesized samples, (b) calcined samples, (c) drug-loaded samples.

Table 1
Structure parameters of mesoporous silica and drug loaded samples

Samples	Lattice structure	Morphology	Particle size	d_{100} (nm)	Pore diameter (nm)	S_{BET} (m^2/g)	V (cm^3/g)	Ibu (wt%) mean ± SD
MCM-41-A	Hexagonal	Sphere	150 nm	3.87	2.0	1580	0.97	
Ibu/MCM-41-A				3.91	1.57	1055	0.90	46.54 ± 2.12
MCM-41-B	Hexagonal	Sphere	500 nm	3.29	1.96	1064	0.69	
Ibu/MCM-41-B				3.29	1.41	771	0.28	26.70 ± 1.53
MCM-41-C	Hexagonal	Sphere	1.25 μm	2.94	2.05	1246	0.89	
Ibu/MCM-41-C				2.98	1.34	824	0.53	39.54 ± 2.44
MCM-41-D	Hexagonal	Sphere	5 μm	4.16	2.45	1138	0.58	
Ibu/MCM-41-D				4.24	1.94	793	0.46	34.32 ± 1.62
MCM-48-E	Cubic	Sphere	500 nm	3.39	2.10	1283	1.51	
Ibu/MCM-48-E				3.29	1.93	717	0.51	45.74 ± 2.01
MCM-41-F	Hexagonal	Rope-like	5–10 μm	4.09	2.25	631	0.76	
Ibu/MCM-41-F				4.16	1.97	470	0.46	35.67 ± 1.57

calcined ones. Therefore, it could be deduced that the pore dimension of the host materials still remained (Fig. 5). These results coincided with the results of XRD patterns. However, as expected, the adsorption capacities decreased due to the presence of the drug molecules. And BET surface area, pore volume, and the average pore diameter were reduced significantly after the drug was loaded (seen in Table 1). These results further proved that the drug has

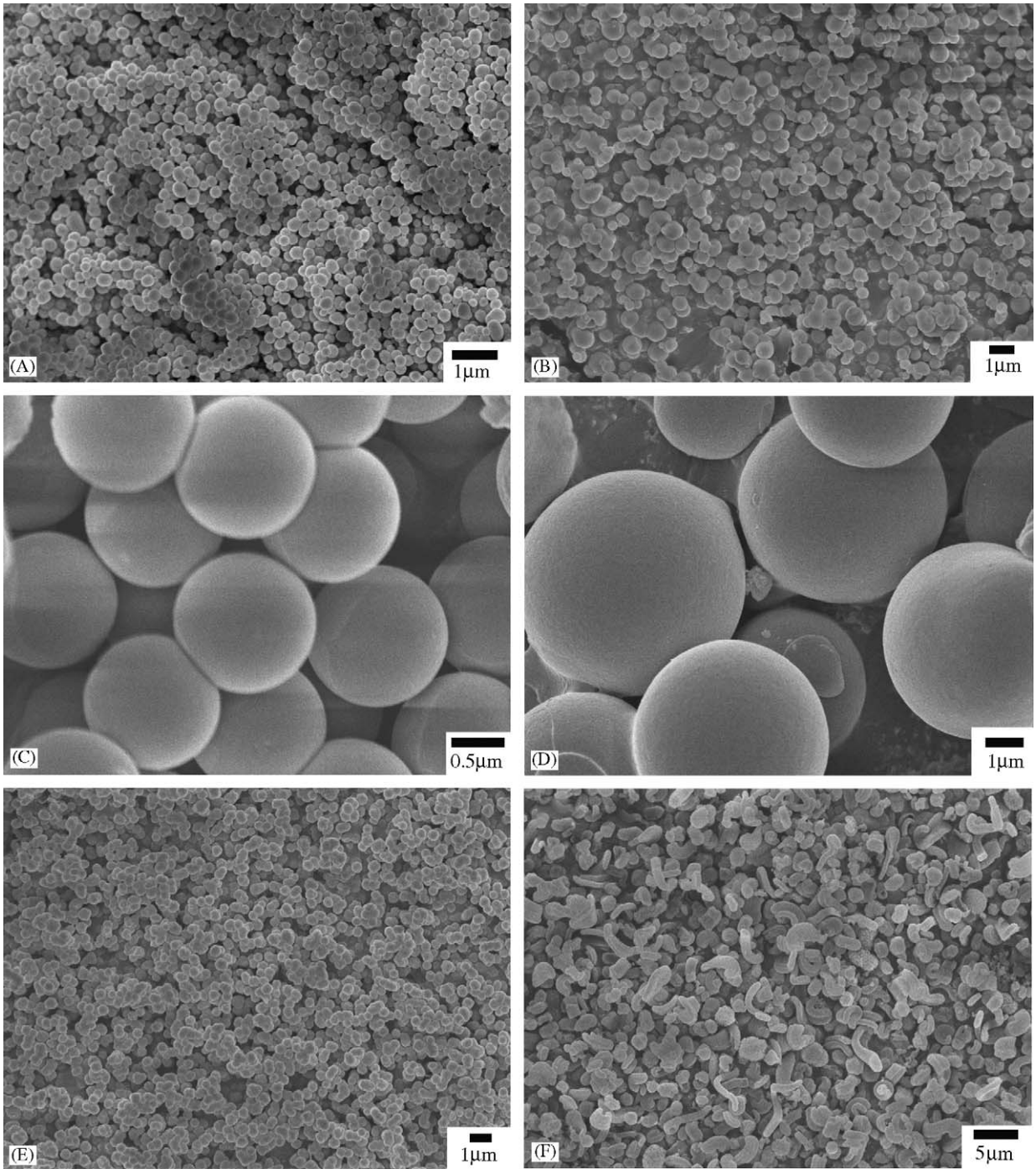

Fig. 2. SEM images of mesoporous silica materials: (A) MCM-41-A, (B) MCM-41-B, (C) MCM-41-C, (D) MCM-41-D, (E) MCM-48-E, and (F) MCM-41-F.

been introduced inside the channel of the mesoporous silica carrier, well consistent with the results of FTIR spectra.

3.2. Drug loading and release profiles

As shown in Table 1, the drug-loading amount has a big difference among different mesoporous silica carriers. Previous study has shown that the drug-loading amount is related to BET surface areas, pore size and surface properties of mesoporous silica [10]. This research has revealed that pore geometry and pore volume could influence the drug-loading amount while the pore size ranged from 1.96 to 2.45 nm as well. The three mesoporous silica carriers employed herein, MCM-41-A, MCM-41-B, and MCM-41-C, have an approximately similar pore size ranging from 1.96 to 2.05 nm; MCM-41-A, with the highest BET surface area ($1580\,m^2/g$) and a large pore volume ($0.97\,cm^3/g$), has the largest drug-loading amount, which is

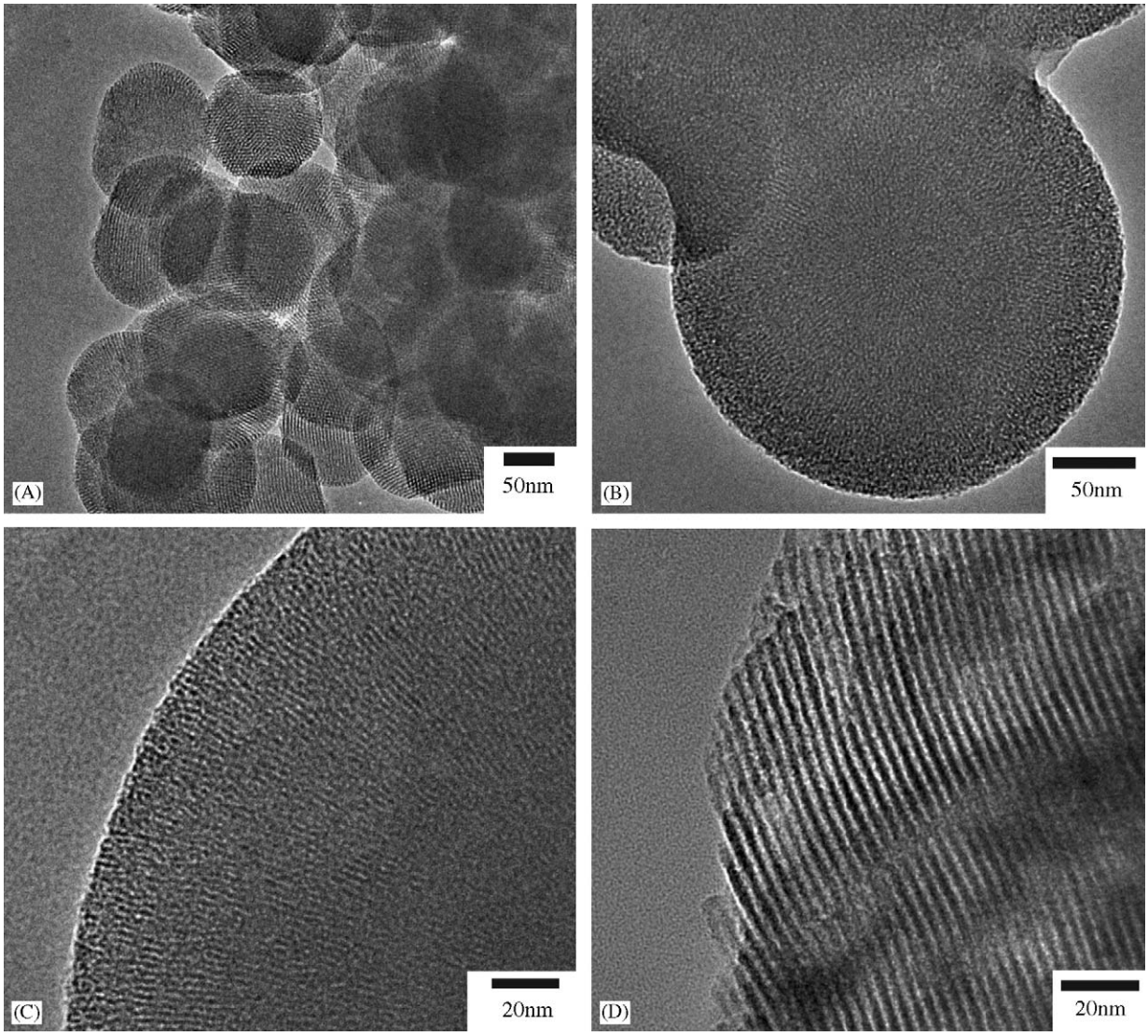

Fig. 3. TEM images of mesoporous silica materials: (A) MCM-41-A, (B) MCM-41-B, (C) MCM-41-C, and (D) MCM-41-F.

up to 46.54 wt%. While for MCM-41-B, with the lowest BET surface ($1064\,m^2/g$) and a small pore volume ($0.69\,cm^3/g$), only 26.70 wt% has been incorporated. And MCM-41-C, with a relatively larger BET surface area ($1246\,m^2/g$), and pore volume ($0.89\,cm^3/g$), the drug-loading amount reaches 39.54 wt%. The significantly larger drug-loading of MCM-48-E may be attributed to its cubic pore geometry of MCM-48-E and large pore volume ($1.51\,cm^3/g$). Comparing MCM-48-E with MCM-41-C, both of them has similar BET surface area and pore size, while the pore volume of MCM-48-E is much larger than that of MCM-41-C, and the pore volume decreased greatly upon loading with the drug (from 1.51 to $0.51\,cm^3/g$). Hence the significantly larger drug-loading of MCM-48-C may be related to its cubic pore geometry and larger pore volume. Whereas MCM-41-F, with a small BET surface area ($631\,m^2/g$) and relatively larger pore volume ($0.764\,cm^3/g$), has a relatively larger drug-loading amount of 35.67 wt%, which implies that there may exist other factors influencing the drug-loading amount besides the factors mentioned above.

The drug release profiles for variable morphologies of mesoporous silica carriers are depicted in Fig. 6. It took 12–84 h to release the majority of ibuprofen from mesoporous materials. It has been found that there is a correlation between the drug release rate and the size of mesoporous silica particles. The MCM-41-A with small spherical particle size of 150 nm shows the fastest drug release rate and displays a total releasing time within 12 h, while the release rates decrease in the sequence of MCM-41-B (500 nm) < MCM-41-C (1.25 μm) < MCM-21-D (5 μm) and, accordingly, it took 36, 48, and 84 h to totally release the drug, respectively. Since the pore diameter and pore surface properties of the mesoporous silica used herein are quite similar, the difference in drug delivery behavior may be reasonably attributed to the influence of the pathway

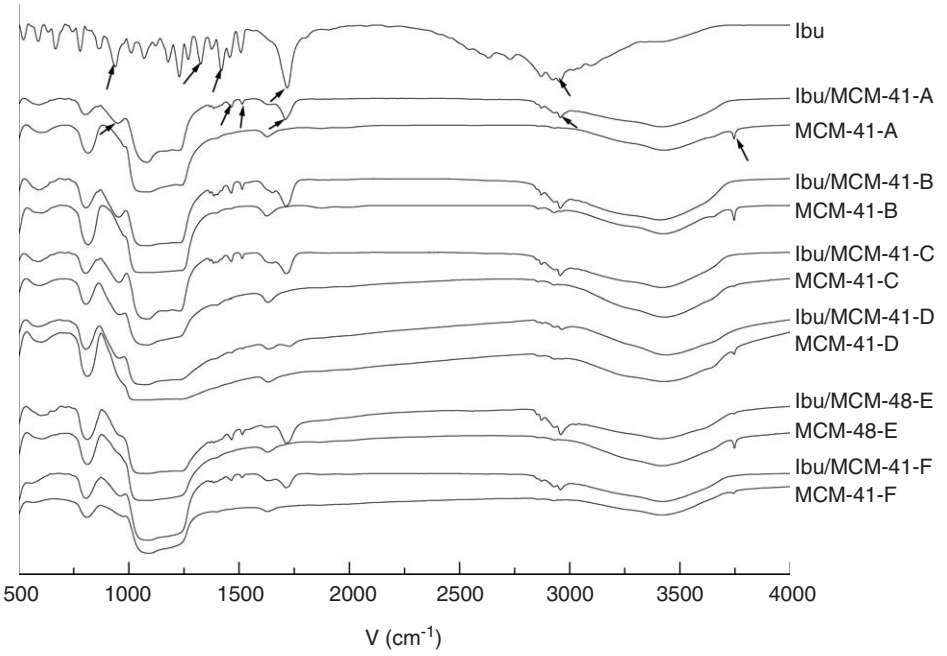

Fig. 4. FTIR spectra of neat ibuprofen, calcined, and drug-loaded mesoporous silica samples.

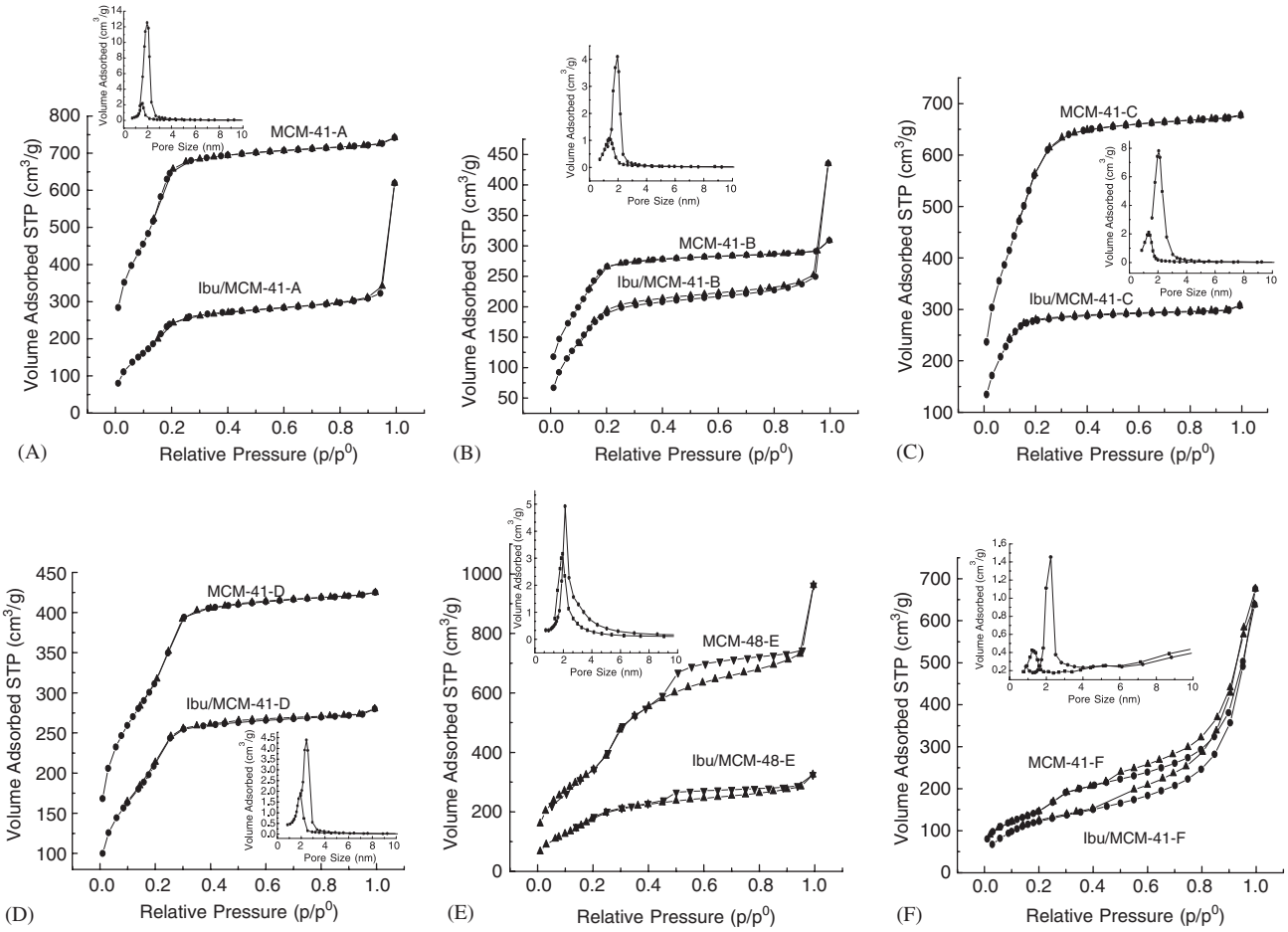

Fig. 5. Nitrogen adsorption/desorption isotherms and corresponding pore size distribution of calcined and drug-loaded samples: (A) MCM-41-A, (B) MCM-41-B, (C) MCM-41-C, (D) MCM-41-D, (E) MCM-48-E, and (F) MCM-41-F.

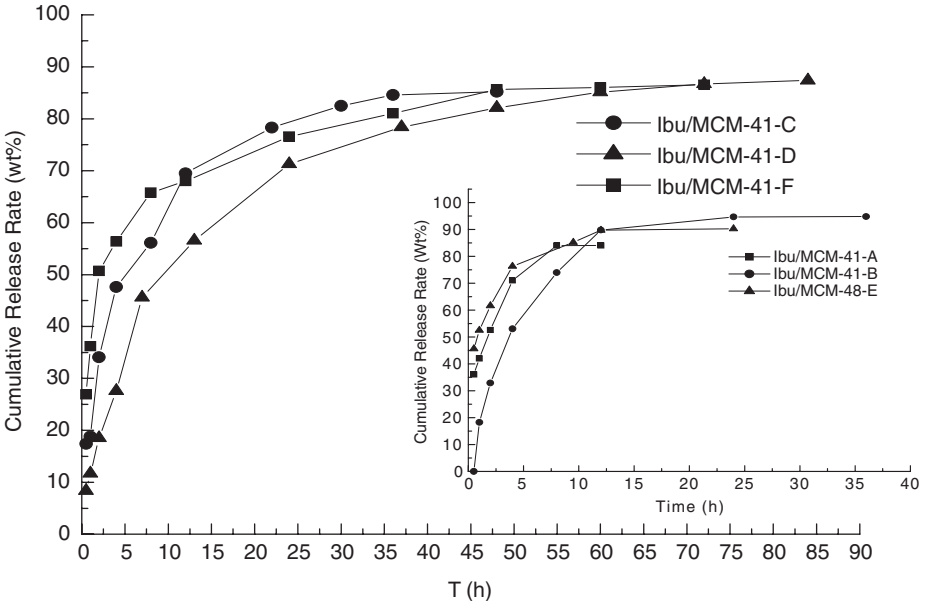

Fig. 6. Cumulative release rates of ibuprofen in simulated body fluid.

(the channel length of the host) of mesoporous silica induced by the morphology. Four mesoporous silica sphere samples, MCM-41-A, MCM-41-B, MCM-41-C, and MCM-41-D, have similar pore diameters in the range of 1.96–2.45 nm, while the channel length may gradually increase with the increase of spherical particle size. The long pathway is unfavorable to the release of drug molecules from the mesopore, which could lead to slow drug release. In addition, there is a large difference in the initial drug release profiles. The Ibu/MCM-41-A delivery system exhibits 42.02 wt% drug-pronounced initial burst release within 1 h, while the amount of drug release from Ibu/MCM-41-B, Ibu/MCM-41-C, and Ibu/MCM-41-D were 18.27, 18.80, and 11.70 wt% within 1 h, respectively. For the cubic MCM-48-E, there were some differences in the drug release profile as compared with that of MCM-41-B. Firstly, the Ibu/MCM-48-E drug delivery system has a larger initial burst release within 2 h than that of Ibu/MCM-41-B. Meanwhile, it could also be found that it took 12 and 24 h to release almost the total drug for Ibu/MCM-48-E and Ibu/MCM-41-B, respectively (Fig. 6). This may be ascribed to the well-massed transportation of the 3D interconnected pore system of MCM-48-E, which is in accordance with the previous report [10]. Therefore, it could be drawn to a conclusion that pore geometry plays an important role on drug delivery profiles in the case of similar pore size and spherical particle size. As for rope-like Ibu/MCM41-F, it has a similar drug delivery profile to that of Ibu/MCM-41-D due to their similar pore diameters and pathways (seen in Table 1). Hence, the length of the pathway induced by morphology must be taken into account, as well as other factors (e.g., pore size, surface chemistry, and pore geometry) when drug delivery behaviors of mesoporous silica carriers were investigated. Our previous research reveals that the water-soluble drug Captopril could be completely released from mesoporous silica carriers [25]. Whereas it should be noted that, unlike the water-soluble drug Captopril, the final drug delivery of ibuprofen could only reach up to ca. 90%, differing from other reports [7,9,10]. Incomplete drug delivery from mesoporous silica carriers may be ascribed to the poor water-solubility of the ibuprofen.

4. Conclusions

A series of mesoporous silica materials with similar pore sizes, variable morphologies, and pore geometries have been employed to control drug delivery under in vitro conditions. It has been revealed that the amount of drug-loading is directly related to the BET surface area, pore geometry, and pore volume of mesoporous silica. Large BET surface area of hexagonal symmetry mesoporous silica carriers usually have large drug-loading amount. Therefore, MCM-41-A, with the highest surface area, has the largest drug-loading amount, which is up to 46.54 wt%. Additionally, cubic MCM-48-E, with large pore volume, also has a large drug-loading amount of 45.74 wt%. The delivery profiles show that the drug release profiles are related to the particle sizes (pathways) induced by their morphologies in the case of the pore diameter in the range of 1.96–2.45 nm. In addition, the pore geometry affects drug delivery profiles as well. Therefore, this study indicates that the morphology must be taken into account while the drug delivery profiles of mesoporous silica carriers are investigated. And the drug release profiles

could be regulated by tailoring the morphology of the mesoporous silica.

Acknowledgments

This work was supported by the National Natural Science Foundation of China (Grant nos. 20571030, 20531030, 29873017 and 20101004), and the State Basic Research Project (G2000077507 and 2003CB615802).

References

[1] K.E. Uhrich, S.M. Cannizzaro, R.S. Langer, K.M. Shakesheff, Chem. Rev. 99 (1999) 3181.
[2] X.P. Qiu, S. Leporatti, E. Donath, H. Möhwald, Langmuir 17 (2001) 5375.
[3] F. Highton, The Pharmaceutics of Ibuprofen, in: K.D. Rainsford (Ed.), Ibuprofen. A Critical Bibliographic Review, Taylor & Francis, London, 1999, p. 53.
[4] Y.L. Cheng, B.G. Trewyn, D.M. Jeftinija, K. Jeftinija, X. Shu, S. Jeftinija, V.S.-Y. Lin, J. Am. Chem. Soc. 125 (2003) 4451.
[5] Q. Fu, G.V.R. Rao, L.K. Ista, Y. Wu, B.P. Andrzejewski, L.A. Sklar, T.L. Ward, G.P. López, Adv. Mater. 15 (15) (2003) 1262.
[6] C. Tourné-Péteilh, D.A. Lerner, C. Charnay, L. Nicole, S. Begu, J.M. Devoisselle, Chem. Phys. Chem 4 (3) (2003) 281.
[7] M. Vallet-Regi, A. Rámila, R.P. del Real, J. Pérez-Pariente, Chem. Mater. 13 (2001) 308.
[8] A. Rámilia, B. Muñoz, J. Pérez-Pariente, M. Vallet-Regí, J. Sol-Gel Sci. Technol. 26 (2003) 1199.
[9] B. Muñoz, A. Rámila, J. Pérez-Pariente, I. Díaz, M. Vallet-Regí, Chem. Mater. 15 (2003) 500.
[10] J. Andersson, J. Rosenholm, S. Areva, M. Lindén, Chem. Mater. 16 (2004) 4160.
[11] P. Horcajada, A. Rámila, J. Pérez-Pariente, M. Vallet-Regí, Microporous Mesoporous Mater. 68 (2004) 105.
[12] Y.F. Zhu, J.L. Shi, W.H. Shen, X.P. Dong, J.W. Feng, M.L. Ruan, Y.S. Li, Angew. Chem. Int. Ed. 44 (2005) 5083.
[13] S.-W. Song, K. Hidajat, S. Kawi, Langmuir 21 (21) (2005) 9568.
[14] S. Liu, P. Cool, O. Collart, P. Van, D. Voort, E.F. Vansant, O.I. Lebeda, G.V. Tendeloo, M. Jiang, J. Phys. Chem. B 107 (2003) 10405.
[15] K. Yano, Y. Fukushima, J. Mater. Chem. 13 (2003) 2577.
[16] L. Qi, J. Ma, H. Cheng, Z. Zhao, Chem. Mater. 10 (1998) 1623.
[17] A. Monnier, F. Schüth, Q. Huo, D. Kumar, D. Margolese, R.S. Maxwell, G.D. Stucky, P. Petroff, A. Firouzi, M. Janicke, B.F. Chmelka, Science 261 (1993) 1299.
[18] S.-E. Günter, R. Jiří, Z.J. Arnošt, J. Inorg. Mater. 1 (1999) 97.
[19] X.S. Zhao, G.Q. Lu, J. Phys. Chem. B 102 (1998) 1556.
[20] C.-Y. Chen, H.-X. Li, M.E. Davis, Microporous Mater. 2 (1993) 17.
[21] L.A. Solovyov, O.V. Belousov, R.E. Dinnebier, A.N. Shmakov, S.D. Kirik, J. Phys. Chem. B 109 (2005) 3233.
[22] J.E. Bateman, R.D. Eagling, D.R. Worrall, B.R. Horrocks, A. Houlton, Angew. Chem. Int. Ed. England 37 (1998) 2683.
[23] P.T. Tanev, T.J. Pinnavaia, Chem. Mater. 8 (1996) 2068.
[24] M. Grün, K.K. Unger, A. Matsumoto, K. Tsutsumi, Microporous Mesoporous Mater. 27 (1999) 207.
[25] F.Y. Qu, G.S. Zhu, S.Y. Huang, S.G. Li, S.L. Qiu, Chem. J. Chinese Univ. 25 (2004) 2195.